

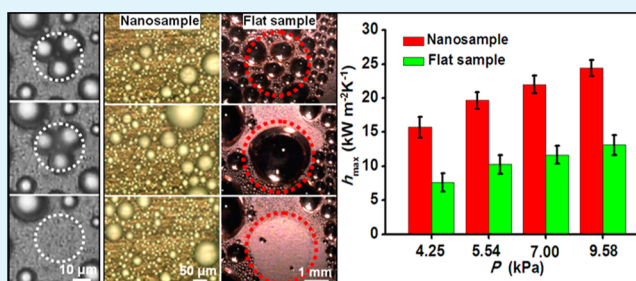
Copper-Based Ultrathin Nickel Nanocone Films with High-Efficiency Dropwise Condensation Heat Transfer Performance

Ye Zhao,[†] Yuting Luo,[†] Jie Zhu, Juan Li, and Xuefeng Gao*

Advanced Thermal Nanomaterials and Devices Research Group, Nanobionic Division, Suzhou Institute of Nano-Tech and Nano-Bionics, Chinese Academy of Sciences, Suzhou 215123, P. R. China

Supporting Information

ABSTRACT: We report a type of copper-based ultrathin nickel nanocone films with high-efficiency dropwise condensation heat transfer (DCHT) performance, which can be fabricated by facile electrodeposition and low-surface-energy chemistry modification. Compared with flat copper samples, our nanosamples show condensate microdrop self-propelling (CMDSP) function and over 89% enhancement in the DCHT coefficient. Such remarkable enhancement may be ascribed to the cooperation of surface nanostructure-induced CMDSP function as well as in situ integration and ultrathin nature of nanofilms. These findings are very significant to design and develop advanced DCHT materials and devices, which help



KEYWORDS: dropwise condensation, nanostructure, ultrathin film, microdrop self-propelling, enhanced heat transfer

Vapor–liquid phase change heat transfer is a type of ubiquitous energy transport way, which is widely used in many fields such as power generation, waste heat utilization, air conditioning, and thermal management.¹ Currently, how to endow metal materials with higher dropwise condensation heat transfer (DCHT) coefficient via surface nanoengineering have attracted great interest because of their extremely important academic and commercial values.^{2–7} Compared with filmwise condensation, dropwise condensation is a type of more efficient heat transfer mode because discrete condensate drops have far lower thermal resistance than continuous liquid films and can release far more bare surface sites for performing more cycles of nucleation, growth and departure.^{8–10} However, condensate drops on the usual flat metal surfaces still have relatively higher thermal resistance, slower renewal frequency, and lower density because they cannot shed off under gravity until growing into the millimeter scale. Recent studies indicated that the DCHT coefficient can be enhanced by a type of innovative condensate microdrop self-propelling (CMDSP) surfaces,^{5–7} which can realize the efficient self-departure of small-scale condensate microdrops via coalescence-released excess surface energy without requiring external forces such as gravity and steam shear force.^{11–19} For example, Miljkovic et al. reported that the DCHT coefficient can be enhanced ~30% by the in situ growth of CMDSP CuO nanoplate films on copper surface.⁵ Very recently, Hou et al. demonstrated that the DCHT coefficient can be enhanced up to ~63% by the smart design of a bionic CMDSP silicon nanoneedle structure inserted with patterned micropillars, which tops are coated by hydrophilic silica so as to increase the density and growth rate of condensates.⁶ However,

such hybrid structure cannot be in situ integrated into metal surfaces, restricted by top-down nanofabrication technologies. Therefore, it is very significant to explore new metal-based nanofilms with higher DCHT coefficient using a facile, cheap, and scalable method.

Here, we report a type of copper-based nickel nanocone films with high-efficiency DCHT performance, which can be achieved by in situ electrodeposition combined with low-surface-energy chemistry modification. Compared with the flat copper samples, our nanosamples own remarkable high-density self-renewal ability to small-scale condensate microdrops. Thermal characterizations indicate that the nanosamples exhibit over 89% enhancement in the DCHT coefficient. Such remarkable enhancement may be ascribed to the cooperation of the surface nanostructure-induced CMDSP function as well as the in situ integration and ultrathin nature of nanofilms. The former can greatly reduce the thermal resistance of condensate drops themselves and increase their renewal frequency and density, whereas the latter can avoid the apparent increment of thermal conduction resistance. These findings are significant to design and develop advanced DCHT nanomaterials and devices, which help improve the efficiency of thermal management and energy utilization.

Figure 1a shows a representative SEM side-view of the as-prepared copper-based nickel nanocone films (for synthesis details, see Experimental Section in the Supporting Informa-

Received: April 15, 2015

Accepted: May 26, 2015

Published: May 26, 2015

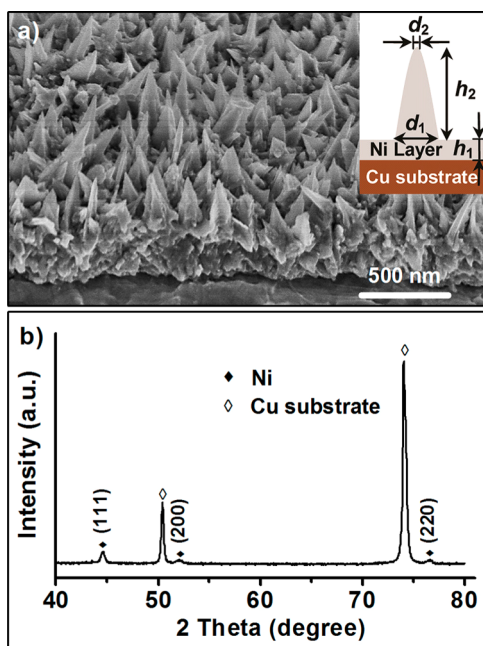


Figure 1. Typical (a) SEM side-view and (b) XRD pattern of the as-prepared copper-based ultrathin nickel nanocone films. The inset in a shows the structure parameters of a simplified nanocone, where h_1 is the thickness of nickel layer, h_2 is the heights of nickel nanocone, and d_1 and d_2 are the base diameter and tip diameter of the nanocone, respectively.

tion). It is evident that the nanocones “stand” on a nickel layer with thickness of ~ 130 nm (h_1), which uniformly covers on the surface of copper substrates. These nanocones have an average diameter of ~ 160 nm at the base (d_1), whereas their sharp tips have an average diameter of ~ 50 nm (d_2). Their average height and apex angle are ~ 400 nm (h_2) and $\sim 33^\circ$, respectively. Figure 1b shows a typical XRD pattern of the as-prepared nanocone films. Evidently, these nanocones are made of pure nickel without other impurities. Three diffraction peaks near 45 , 52 , and 76° can be indexed as the crystal face (111), (200), and (220) of face-centered cubic nickel (see JCPDS File No. 040850). Because of the ultrathin nature of the as-prepared nanocone films, the signal intensity of nickel detected is apparently weaker than that of copper originating from the substrates.

After low-surface-energy modification, the nanocone films show typical superhydrophobicity for deposited macroscopic big-scale water drops (Figure S1 in the Supporting Information) and condensate microdrops. Figure 2a shows a microscopic optical image of a spherical condensate microdrop on the nanosample surface. Its contact angle is $164.3 \pm 2.6^\circ$. No doubt that the solid–liquid contact area and interface adhesion between the suspended microdrop and the nanosample surface should be extremely low.^{17–21} To explore the self-transport ability of condensate microdrops on the nanosample surfaces, we placed them on a vertical cooling stage with substrate temperature of $\sim 2^\circ\text{C}$, ambient temperature of $\sim 26^\circ\text{C}$, and relative humidity of $\sim 90\%$. Evidently, adjacent condensate microdrops can self-remove via their mutual coalescence (Figure 2b), triggered by direct condensation growth. Figure 2c shows a trajectory of a merged microdrop ejecting from the nanosample surface. Our previous studies have revealed that the tip-like nanostructures with extremely low interface adhesion can minimize the dissipation of

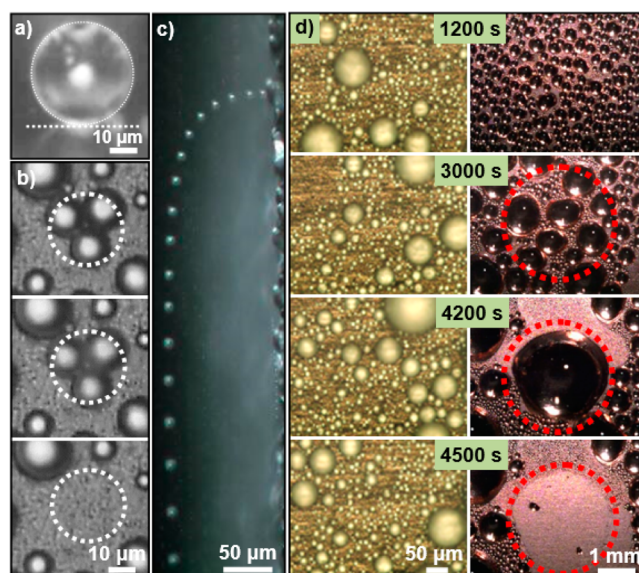


Figure 2. (a) Optical image of a spherical condensate microdrop on the nanosample surface, showing a static contact angle of $\sim 161^\circ$. (b) Optical top-views showing coalescence-induced condensate microdrop self-departure on the vertical nanosample surface. (c) Overlapped optical side-view showing the trajectory of a merged microdrop ejecting from the nanosample surface. (d) Time-lapse optical images showing distinct condensation events on the vertical nanosample (left) and flat (right) sample.

coalescence-released weak surface energy so as to ensure the efficient self-departure of condensate microdrops.¹⁷ As a result, the nanosample surface can always maintain high-density self-renewal of small-scale condensate microdrops during the whole condensation process (as shown in the left of Figure 2d), whereas condensate drops on the flat copper surfaces only can shed off under gravity until they grow into the millimeter scale (right of Figure 2d). Clearly, reducing the departure sizes of condensate drops from the millimeter scale to the micrometer can greatly shorten their residence period and release more surface sites for performing more cycles of nucleation, growth and departure.

To quantify and highlight the dropwise condensation property of our nanosamples at the microscale, we further analyze the drop number distribution of residence microdrops with diameters (d) of <10 μm , 10 – 50 μm and 50 – 100 μm (Figure 3a). Microdrops with $d < 10$ μm dominate on the nanosample surface, occupying over 80% during the whole condensation process despite presenting slight fluctuation (Figure 3a, top panel); microdrops with $d = 10$ – 50 μm ($d > 50$ μm) can form after ~ 300 s (~ 700 s), occupying 5–10% ($< 5\%$). In contrast, the diameters of condensate drops on the flat surface can rapidly increase over 100 μm within shorter duration (~ 400 s) and the number of condensate microdrops can gradually reduce with the time extending (Figure 3a, bottom panel). Compared with flat surface, our nanosamples can efficiently control the departure sizes of condensate drops at the microscale, especially below 10 μm , during the whole condensation process. As a result, the nanosample surface can always maintain higher microdrop density (Figure 3b), presenting an average of $\sim 3.14 \times 10^3$ mm^{-2} . In sharp contrast, the density of condensate drops on flat surfaces is apparently lower and gradually declines with the time extending. Clearly,

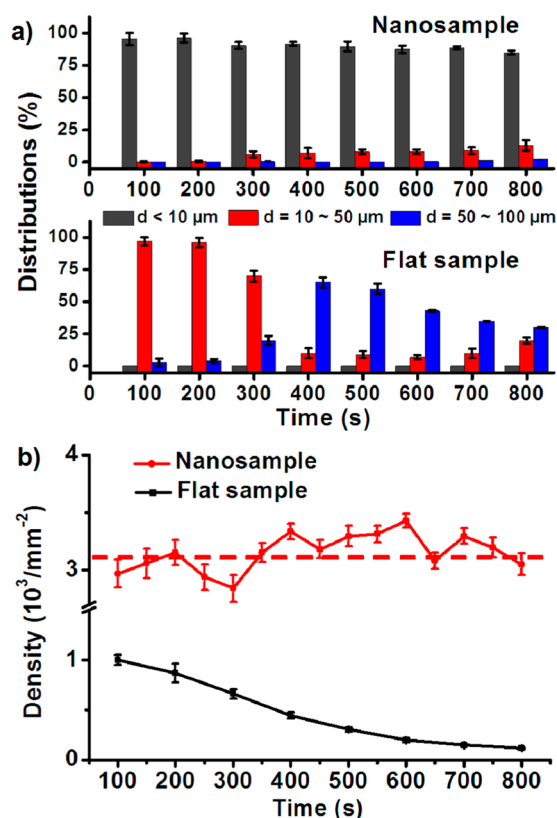


Figure 3. (a) Drop number distribution of condensate microdrops with diameters (d) of <10 , $10\text{--}50$, and $50\text{--}100 \mu\text{m}$ on the vertical nanosamples (top) and flat samples (bottom) varied with time. (b) Density of condensate drops on the nanosamples (red) and flat samples (black) varied with time.

the copper-based nickel nanocone films own remarkable CMDSP function.

In principle, such copper-based nickel nanocone film with CMDSP function should possess high-efficiency DCHT performance. Generally, the DCHT coefficient can be measured by a custom-tailored setup (details see Figure S2 in the Supporting Information). Figure 4a shows a measuring principle diagram. To ensure one-dimensional axial steady-state heat transfer model, we inserted a fin-integrated cylindrical copper block (Figure S3 in the Supporting Information) into a Teflon insulator that divides a steel chamber into a condensation chamber (right) and a cooling chamber (left). Via regulating the pressure (P) of saturated vapor (with the corresponding temperature, T_v) and the temperature of coolant (with a fixed flow rate), we can measure the temperature gradient (∇T) within copper block using equidistant thermocouples, which can be used for calculating the surface temperature (T_s). As a result, the DCHT coefficient (h) of the samples can be obtained by the equation $h = k\nabla T/\Delta T$, where k is the thermal conductivity of copper and ΔT is the degree of wall subcooling (i.e., the difference between T_v and T_s). Figure 4b shows the DCHT coefficient of the nanosamples and contrast flat samples under varied P while fixing $\Delta T = 1.3 \pm 0.1$ K. The DCHT coefficient of the nanosample is apparently higher than that of the flat samples and can increase with the increase of P . The calculated enhancement factors, defined as $(h_{\text{nano}} - h_{\text{flat}})/h_{\text{flat}}$, are ~ 1.1 (as $P = 4$ kPa), ~ 1.06 (as $P = 5.54$ kPa), ~ 0.95 (as $P = 7.00$ kPa) and ~ 0.89 (as $P = 9.58$ kPa), respectively. Clearly, the DCHT coefficient of copper surfaces

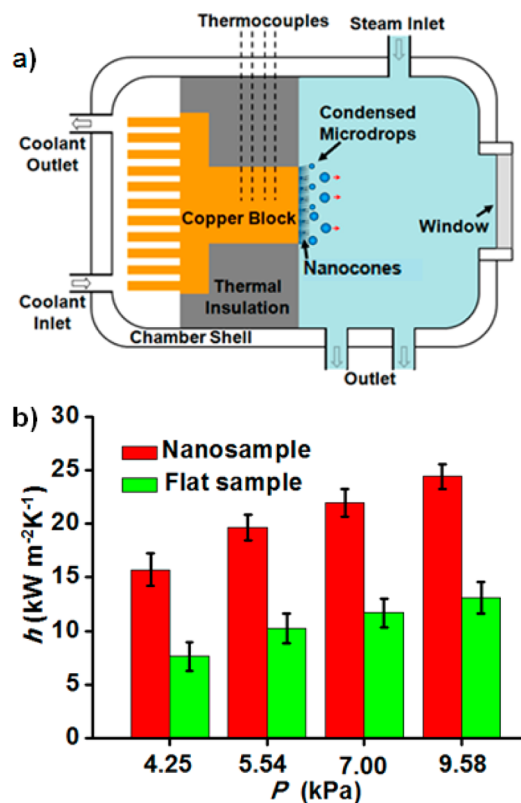


Figure 4. (a) Principle diagram of measuring the dropwise condensation heat transfer (DCHT) coefficient. (b) DCHT coefficients (h) of the nanosamples (red) and contrast flat samples (green) under varied saturated vapor pressure (P).

can be enhanced over 89% via the in situ growth of nickel nanocone films.

Why does such a copper-based nickel nanocone film own high-efficiency DCHT performance? We suppose that this may be ascribed to the following three reasons. First, our nanosample can realize efficient self-removal of small-scale condensate microdrops. With the departure sizes of condensate drops reducing from the millimeter scale to the micrometer, the thermal resistance of residence drops themselves can be greatly reduced. Second, the efficient self-removal of condensate microdrops means faster renewal frequency of residence drops and more releasable bare surface sites for performing more cycles of nucleation, growth, and departure, which are also very beneficial to enhance the DCHT coefficient per unit area and time. In sharp contrast, condensate drops on the flat surfaces not only have higher thermal resistance but have lower renewal frequency and density, which are highly disadvantageous to the efficient transport of latent heat released from steam condensation. Third, the in situ integration and ultrathin nature of functional nanofilms are also crucial to ensure the high-efficiency DCHT.²² It is well-known that the introduction of nanofilms inevitably brings about additional thermal conduction resistance for metal materials. Compared with the usual adhesion way of adopting thermal conductive glues, the in situ integration way can effectively reduce interface thermal resistance between the nanofilm and the metal substrate. In addition, our ultrathin nanofilms with thickness of merely ~ 500 nm may avoid the apparent increment of thermal conduction resistance. Clearly, it is just the cooperation of these effects that endow the copper-based nickel nanocone films with superior

DCHT performance. Note that it is extremely difficult to capture the microscopic mass-transfer details during the thermal characterization process and the high-resolution imaging of microdrop-nanostructure interactions in the ambient condition is still useful to reveal the nanostructure effects on the DCHT enhancement.

In conclusion, we report a type of copper-based ultrathin nickel nanocone films with high-efficiency DCHT performance, which can be achieved by facile electrodeposition combined with low-surface-energy chemistry modification. Such superior performance may be ascribed to the cooperation of surface nanostructure-induced CMDSP function as well as in situ integration and ultrathin nature of nanofilms. The former can greatly reduce the thermal resistance of condensate drops themselves and increase their renewal frequency and density while the latter can avoid the apparent increment of thermal conduction resistance. These findings are significant to design and develop advanced DCHT nanomaterials and devices, which help improve the efficiency of thermal management and energy utilization. Our method is promising to be evolved into a type of industry-compatible technologies applicable to metal-based surface nanoengineering in a facile, inexpensive, and scalable way. In addition, the ultrathin nickel nanocone films may be multifunctional because they can find a variety of nanotechnological applications, e.g., moisture self-cleaning,²³ antifrosting,^{24–27} electrostatic energy harvesting,²⁸ anticorrosion,²⁹ and used as conventional superhydrophobic coatings referring to macroscopic drops.³⁰

■ ASSOCIATED CONTENT

Supporting Information

Experimental Section, ideal superhydrophobicity to macroscopic water droplets (Figure S1), schematic of the custom design condensation heat transfer characterization setup (Figure S2), optical image and outline dimension drawing of a copper block (Figure S3), the recorded heat flux varied as the degree of surface subcooling (Figure S4), the crucial parameters during the condensation heat transfer measurements (Table S1). The Supporting Information is available free of charge on the ACS Publications website at DOI: 10.1021/acsami.5b03264.

■ AUTHOR INFORMATION

Corresponding Author

*E-mail: xfgao2007@sinano.ac.cn.

Author Contributions

†Y.Z and Y.L. contributed equally.

Notes

The authors declare no competing financial interest.

■ ACKNOWLEDGMENTS

This work was supported by the National Basic Research Program of China (2012CB933200), Key Research Program of the Chinese Academy of Sciences (KJZD-EW-M01), National Natural Science Foundation of China, Collaborative Innovation Center of Suzhou Nano Science & Technology, and Suzhou Institute of Nano-Tech and Nano-Bionics, CAS.

■ REFERENCES

(1) Carey, V. P. *Liquid-Vapor Phase-Change Phenomena*; Taylor and Francis: London, 2008.

(2) Miljkovic, N.; Wang, E. N. Condensation Heat Transfer on Superhydrophobic Surfaces. *MRS Bull.* **2013**, *38*, 397–406.

(3) Enright, R.; Miljkovic, N.; Alvarado, J. L.; Kim, K.; Rose, J. W. Dropwise Condensation on Micro and Nanostructured Surfaces. *Nanoscale Microscale Thermophys. Eng.* **2014**, *18*, 223–250.

(4) Boreyko, J. B.; Zhao, Y. J.; Chen, C.-H. Planar Jumping-Drop Thermal Diodes. *Appl. Phys. Lett.* **2011**, *99*, 234105.

(5) Miljkovic, N.; Enright, R.; Nam, Y.; Lopez, K.; Dou, N.; Sack, J.; Wang, E. N. Jumping-Droplet-Enhanced Condensation on Scalable Superhydrophobic Nanostructured Surfaces. *Nano Lett.* **2013**, *13*, 179–187.

(6) Hou, Y.; Yu, M.; Chen, X.; Wang, Z.; Yao, S. Recurrent Filmwise and Dropwise Condensation on a Beetle Mimetic Surface. *ACS Nano* **2015**, *9*, 71–81.

(7) Zhu, J.; Luo, Y.; Tian, J.; Li, J.; Gao, X. Clustered Ribbed-Nanoneedle Structured Copper Surfaces with High-Efficiency Dropwise Condensation Heat Transfer Performance. *ACS Appl. Mater. Interfaces* **2015**, *7*, 10660–10665.

(8) Schmidt, E.; Schurig, W.; Sellschopp, W. Versuche über die Kondensation von Wasserdampf in Film- und Tropfenform. *Forsch. Ingenieurwes.* **1930**, *1*, 53–63.

(9) Rose, J. W. Dropwise Condensation Theory and Experiment: A Review. *Proc. Inst. Mech. Eng. Part A* **2002**, *216*, 115–128.

(10) Daniel, S.; Chaudhury, M. K.; Chen, J. C. Fast Drop Movements Resulting from the Phase Change on a Gradient Surface. *Science* **2001**, *291*, 633–636.

(11) Chen, C.-H.; Cai, Q.; Tsai, C.; Chen, C.-L.; Xiong, G.; Yu, Y.; Ren, I. Dropwise Condensation on Superhydrophobic Surfaces with Two-Tier Roughness. *Appl. Phys. Lett.* **2007**, *90*, 173108.

(12) Boreyko, B.; Chen, C.-H. Self-Propelled Dropwise Condensate on Superhydrophobic Surfaces. *Phys. Rev. Lett.* **2009**, *103*, 184501.

(13) Feng, J.; Qin, Z.; Yao, S. Factors Affecting the Spontaneous Motion of Condensate Drops on Superhydrophobic Copper Surfaces. *Langmuir* **2012**, *28*, 6067–6075.

(14) Feng, J.; Pang, Y.; Qin, Z.; Ma, R.; Yao, S. Why Condensate Drops Can Spontaneously Move Away on Some Superhydrophobic Surfaces but Not on Others. *ACS Appl. Mater. Interfaces* **2012**, *4*, 6618–6625.

(15) He, M.; Zhou, X.; Zeng, X.; Cui, D.; Zhang, Q.; Chen, J.; Li, H.; Wang, J.; Cao, Z.; Song, Y.; Jiang, L. Hierarchically Structured Porous Aluminum Surfaces for High-Efficient Removal of Condensed Water. *Soft Matter* **2012**, *8*, 6680–6683.

(16) He, M.; Zhang, Q.; Zeng, X.; Cui, D.; Chen, J.; Li, H.; Wang, J.; Song, Y. Hierarchical Porous Surface for Efficiently Controlling Microdroplets' Self-Removal. *Adv. Mater.* **2013**, *25*, 2291–2295.

(17) Tian, J.; Zhu, J.; Guo, H.-Y.; Li, J.; Feng, X.-Q.; Gao, X. Efficient Self-Propelling of Small-Scale Condensed Microdrops by Closely-Packed ZnO Nanoneedles. *J. Phys. Chem. Lett.* **2014**, *5*, 2084–2088.

(18) Luo, Y.; Li, J.; Zhu, J.; Zhao, Y.; Gao, X. Fabrication of Condensate Microdrop Self-Propelling Porous Films of Cerium Oxide Nanoparticles on Copper Surfaces. *Angew. Chem., Int. Ed.* **2015**, *54*, 4876–4879.

(19) Zhao, Y.; Luo, Y.; Li, J.; Yin, F.; Zhu, J.; Gao, X. Condensate Microdrop Self-Propelling Aluminum Surfaces Based on Controllable Fabrication of Alumina Rod-Capped Nanopores. *ACS Appl. Mater. Interfaces* **2015**, DOI: 10.1021/acsami.5b03016.

(20) Lai, Y.; Gao, X.; Zhuang, H.; Huang, J.; Lin, C.; Jiang, L. Designing Superhydrophobic Porous Nanostructures with Tunable Water Adhesion. *Adv. Mater.* **2009**, *21*, 3799–3803.

(21) Tian, J.; Zhang, Y.; Zhu, J.; Yang, Z.; Gao, X. Robust Nonsticky Superhydrophobicity by the Tapering of Aligned ZnO Nanorods. *ChemPhysChem* **2014**, *15*, 858–861.

(22) Miljkovic, N.; Enright, R.; Wang, E. N. Modeling and Optimization of Superhydrophobic Condensation. *J. Heat Transfer* **2013**, *135*, 111004.

(23) Wisdom, K. M.; Watson, J. A.; Qu, X.; Liu, F.; Watson, G. S.; Chen, C.-H. Self-Cleaning of Superhydrophobic Surfaces by Self-Propelled Jumping Condensate. *Proc. Natl. Acad. Sci. U. S. A.* **2013**, *110*, 7992–7997.

(24) Chen, X.; Ma, R.; Zhou, H.; Zhou, X.; Che, L.; Yao, S.; Wang, Z. Activating the Microscale Edge Effect in a Hierarchical Surface for Frosting Suppression and Defrosting Promotion. *Sci. Rep.* **2013**, *3*, 2515.

(25) Lv, J.; Song, Y.; Jiang, L.; Wang, J. Bio-Inspired Strategies for Anti-Icing. *ACS Nano* **2014**, *8*, 3152–3169.

(26) Xu, Q.; Li, J.; Tian, J.; Zhu, J.; Gao, X. Energy-Effective Frost-Free Coatings Based on Superhydrophobic Aligned Nanocones. *ACS Appl. Mater. Interfaces* **2014**, *6*, 8976–8980.

(27) Hao, Q.; Pang, Y.; Zhao, Y.; Zhang, J.; Feng, J.; Yao, S. Mechanism of Delayed Frost Growth on Superhydrophobic Surfaces with Jumping Condensates: More Than Interdrop Freezing. *Langmuir* **2014**, *30*, 15416–15422.

(28) Milkovic, N.; Preston, D. J.; Enright, R.; Wang, E. N. Jumping-Droplet Electrostatic Energy Harvesting. *Appl. Phys. Lett.* **2014**, *105*, 013111.

(29) Liu, Y.; Yin, X.; Zhang, J.; Yu, S.; Han, Z.; Ren, L. A Electro-Deposition Process for Fabrication of Biomimetic Super-Hydrophobic Surface and Its Corrosion Resistance on Magnesium Alloy. *Electrochim. Acta* **2014**, *125*, 395–403.

(30) Tian, Y.; Su, B.; Jiang, L. Interfacial Material System Exhibiting Superwettability. *Adv. Mater.* **2014**, *26*, 6872–6897.